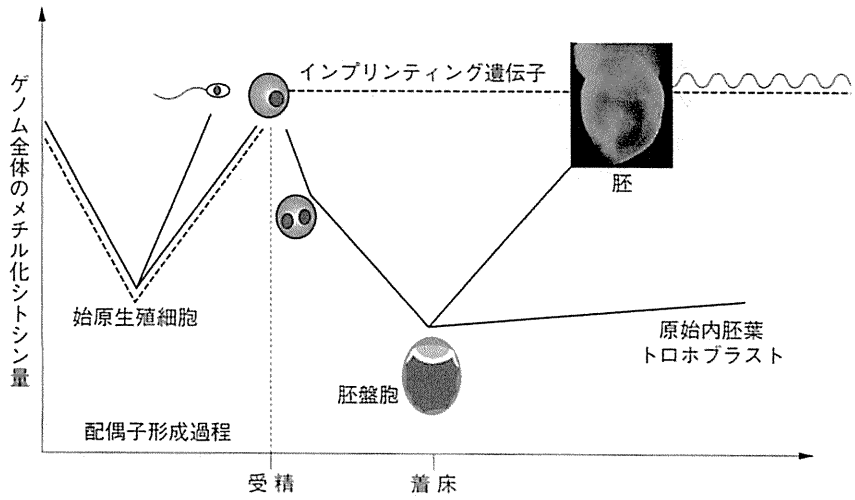

図２　発生過程におけるDNAメチル化状態の変化

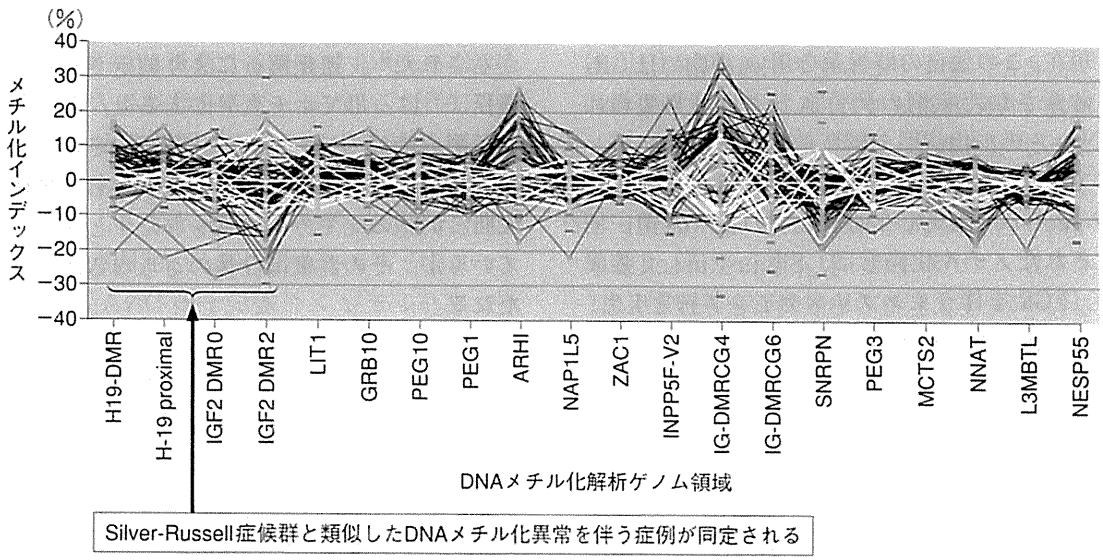

図３　FGR（IUGR）症例の胎盤DNAメチル化解析例

子由来の胚では，一部の領域で異常なDNAメチル化消失が起きている。正常胚では，これらの遺伝子が，これらの領域を生理的脱メチル化からブロックしていると考えられる[12]。

本節で述べた見解はすべてモデル動物の解析結果であり，必ずしもすべてヒトと同一ではない可能性があるが，ヒト初期胚を系統的に調べることは困難であり，今後もこれらの知見が，産科異常のエピジェネティクスを解析する際の重要な手掛かりとなるであろう。

V. 胎児発育のエピジェネティクス

ここまで示してきたように，エピジェネティックな遺伝子発現制御は，生殖や発生において重要な役割を担っていることが，様々なモデル動物の解析から示されている。特に，インプリンティング異常疾患（前述のSilver-Russell症候群やBeckwith-Wiedemann症候群など）の例から，ゲノムインプリンティングが破綻すれば，ヒトでも胎児発育異常を呈するこ

とを述べた。それでは逆に，FGR（IUGR）と診断された症例には，エピジェネティックな異常を伴う症例が存在しているのであろうか。

われわれは現在，「胎児や胎盤の発生分化・発育異常を呈する異常妊娠には，未知のゲノムインプリンティング異常，DNA メチル化異常などのエピジェネティクス異常を伴う症例が存在する」という仮説の下に研究を進めている。エピジェネティックな修飾状態を効率よくスクリーニングするために，ヒトインプリンティング遺伝子の調節領域，胎児胎盤の発生発育に深く関与していると考えられている領域を，過去の報告あるいはマウスゲノムとの比較により網羅的に抽出し，DNA メチル化状態を定量評価する解析系を独自に確立した（図 3，中林ら未発表データ）。

現在，この独自の解析系を用い，FGR（IUGR）と診断された症例の臍帯血および胎盤組織の DNA メチル化状態を網羅的に解析している。すでに解析を終えた百余症例から，2 症例に DNA メチル化異常を同定している（図 3）。同定されたメチル化異常は，Silver-Russell 症候群（FGR を伴うインプリンティング異常疾患）でも報告されている領域の低 DNA メチル化であることから，これらの FGR（IUGR）発症には，共通の分子病態が存在すると推測される。

また，これらの症例では，DNA メチル化異常は胎盤ゲノム DNA のみに認められ，同一児の臍帯血ゲノム DNA には認められなかった。発生学的な考察から，このような DNA メチル化異常が起こるとすれば，その起源は親の配偶子ではなく，受精後の，胚体外組織と胚体組織が非可逆的に分化した時点，おそらく胚盤胞期前後であろうと推測される。加えて，DNA メチル化異常が局所的であることから，DNA メチル化機構の異常による系統的な消失ではなく，偶発的なメチル化消失であることが示唆される。よって，今回われわれが同定した症例に関しては，出生後に DNA メチル化異常に起因する生理機能異常は伴わず，同胞や次世代に同様の異常が発生する可能性は極めて低いであろう，という予測が立つ。諸家からの報告も，解析対象領域と結論が限定的ではあるが，われわれの結果と矛盾しない程度の頻度でメチル化異常症例を検出している[13)~16)]。

そのほか，最近同定されたエピジェネティックな異常を伴うヒト発生異常疾患として，反復胞状奇胎が挙げられる。通常の完全胞状奇胎は雄核発生であり，父親の染色体のみを有する。ところが反復胞状奇胎は，組織学的には通常の完全胞状奇胎とまったく同一であるにもかかわらず，非常に奇妙なことに，両親由来の染色体を有する一見正常な二倍体である。同疾患の発症機序に多大な関心が寄せられていたが，その後の詳細な解析により，反復胞状奇胎組織は，正常な二倍体ではあるものの，インプリンティング遺伝子の DNA メチル化を失っていることが示された[17)]。連鎖解析により同定された原因遺伝子[18)]に，母でホモ変異があると，おそらく卵子形成時に DNA メチル化が確立されず，ゲノムインプリンティングに異常が生じ，雄核発生胚と同様の発生分化異常をきたすと考えられているが，その詳細は今後のさらなる解析が待たれる。

VI. 環境による胎児のエピジェネティックな変化

ここまで，産科領域に関係する生理的なエピジェネティクスあるいはその破綻による疾患について述べてきたが，最後に，母体環境による胚のエピジェネティックな変化をモデル生物で解析した例を紹介する。

マウスの体毛の色を決める遺伝子に viable yellow agouti と呼ばれる変異があると，兄弟間で文字どおり黄色から野生色まで様々な毛色を持つ個体が生まれてくる。この変異では，毛色を決める遺伝子の近くにトランスポゾンと呼ばれる配列が挿入されており，その挿入配列が DNA メチル化によって抑制されていると通常の野生色になり，逆に DNA メチル化の程度が低いと黄色くなる。母体に，妊娠前から授乳期

まで葉酸やビタミン B_{12} など（代謝産物がメチル基の供与体となるもの）を過剰摂取させ続けると，生まれてくる子どもは高い頻度で野生色を呈するようになる。予想どおり，これらの子どもでは挿入配列が高度にメチル化され，しかもその状態が成獣になっても維持されていた[19]。母体の食餌による胎児期の環境が，胎児のDNAメチル化状態に影響を与え，出生後も長期にわたり遺伝子発現を変化させたと考えられる。この実験結果の解釈には慎重を期さねばならないが，少なくとも「環境要因が除去されても影響が長期にわたって遺残する現象」に，エピジェネティックな分子メカニズムが介在している可能性は十分に考えられ，今後の検証が待たれる。

おわりに

以上，本稿では，産科領域に深くかかわっているエピジェネティックな遺伝子発現制御を簡潔に紹介してきた。産科疾患を丁寧に解析していくことで，産科異常の病態解明のみならず，実験が困難なヒト初期発生における分化制御機構の解明が期待される。得られる基盤的知見は，再生医療や腫瘍性疾患の研究にも貢献できるものと考える。また，本稿ではジェネティックな解析については割愛したが，エピジェネティックな生命現象の理解が深まるにつれ，なおさらのこととしてジェネティックな解析も併せて行い，ゲノム機能を多面的にとらえる研究が今後はますます重要になってくると予想される。

謝辞：われわれの研究部で行った異常妊娠のDNAメチル化解析は，中林一彦合併症妊娠管理室長が実験系を確立し，九州大学産婦人科山口裕子，千葉大学大学院生鳥巣弘道らが中心に解析を行った。また，臨床検体は，国立成育医療研究センター周産期診療部，九州大学医学部産婦人科，社会保険相模野病院産婦人科からご提供いただいた。

文　献

1) McGrath J, Solter D : Completion of mouse embryogenesis requires both the maternal and paternal genomes. Cell, **37** : 179-183, 1984.
2) Surani MA, Barton SC, Norris ML : Development of reconstituted mouse eggs suggests imprinting of the genome during gametogenesis. Nature, **308** : 548-550, 1984.
3) Bourc'his D, Xu GL, Lin CS, et al : Dnmt3L and the establishment of maternal genomic imprints. Science, **294** : 2536-2539, 2001.
4) Hata K, Okano M, Lei H, et al : Dnmt3L cooperates with the Dnmt3 family of *de novo* DNA methyltransferases to establish maternal imprints in mice. Development, **129** : 1983-1993, 2002.
5) Bourc'his D, Bestor TH : Meiotic catastrophe and retrotransposon reactivation in male germ cells lacking Dnmt3L. Nature, **431** : 96-99, 2004.
6) Hata K, Kusumi M, Yokomine T, et al : Meiotic and epigenetic aberrations in Dnmt3L-deficient male germ cells. Mol Reprod Dev, **73** : 116-122, 2006.
7) Tachibana M, Nozaki M, Takeda N, et al : Functional dynamics of H3K9 methylation during meiotic prophase progression. EMBO J, **26** : 3346-3359, 2007.
8) Kuramochi-Miyagawa S, Kimura T, Ijiri TW, et al : Mili, a mammalian member of piwi family gene, is essential for spermatogenesis. Development, **131** : 839-849, 2004.
9) Kuramochi-Miyagawa S, Watanabe T, Gotoh K, et al : DNA methylation of retrotransposon genes is regulated by Piwi family members MILI and MIWI2 in murine fetal testes. Genes Dev, **22** : 908-917, 2008.
10) Marques CJ, Carvalho F, Sousa M, et al : Genomic imprinting in disruptive spermatogenesis. Lancet, **363** : 1700-1702, 2004.
11) Kobayashi H, Sato A, Otsu E, et al : Aberrant DNA methylation of imprinted loci in sperm from oligospermic patients. Hum Mol Genet, **16** : 2542-2551, 2007.
12) Nakamura T, Arai Y, Umehara H, et al : PGC7/Stella protects against DNA demethylation in early embryogenesis. Nat Cell Biol, **9** : 64-71, 2007.
13) Bourque DK, Avila L, Penaherrera M, et al : Decreased placental methylation at the H19/IGF2 imprinting control region is associated with normotensive intrauterine growth restriction but not preeclampsia. Placenta, **31** : 197-202,

2010.
14) Lambertini L, Diplas AI, Lee MJ, et al : A sensitive functional assay reveals frequent loss of genomic imprinting in human placenta. Epigenetics, **3** : 261-269, 2008.
15) McMinn J, Wei M, Schupf N, et al : Unbalanced placental expression of imprinted genes in human intrauterine growth restriction. Placenta, **27** : 540-549, 2006.
16) Guo L, Choufani S, Ferreira J, et al : Altered gene expression and methylation of the human chromosome 11 imprinted region in small for gestational age (SGA) placentae. Dev Biol, **320** : 79-91, 2008.
17) Judson H, Hayward BE, Sheridan E, et al : A global disorder of imprinting in the human female germ line. Nature, **416** : 539-542, 2002.
18) Murdoch S, Djuric U, Mazhar B, et al : Mutations in NALP7 cause recurrent hydatidiform moles and reproductive wastage in humans. Nat Genet, **38** : 300-302, 2006.
19) Waterland RA, Jirtle RL : Transposable elements : targets for early nutritional effects on epigenetic gene regulation. Mol Cell Biol, **23** : 5293-5300, 2003.

学会案内

第114回日本産科麻酔学会

日　　時：平成22年12月4日（土）午前10時より（予定）
開催場所：横浜シンポジア
　　横浜市中区山下町2番地　産業貿易センター9階　045-671-7151
一般演題・教育講演：一般演題の申込は事務局へお問い合わせ下さい。
演題締切り：平成22年10月31日（日）必着

日本産科麻酔学会事務局：
北里大学病院産婦人科（内）
〒252-0375 神奈川県相模原市南区北里1-15-1
TEL：042-778-8414　FAX：042-778-9433
E-mail Address：jsoap@med.kitasato-u.ac.jp

発達障害の診療に携わる医師、コメディカル・スタッフ必読!!

発達障害 子どもを診る医師に 知っておいてほしいこと

日常診療、乳幼児健診から対応まで

医学博士 平岩 幹男 著

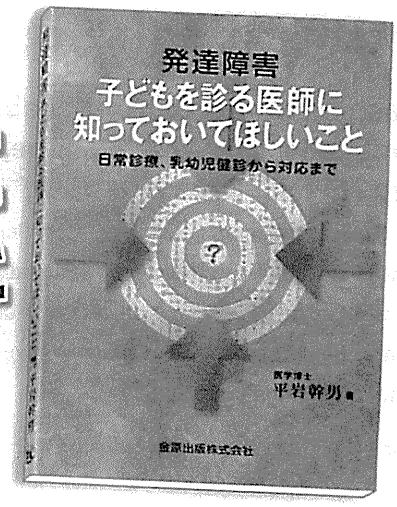

A5判 200頁 12図 ISBN978-4-307-17059-8
定価2,940円(本体2,800円+税5%)

"子どもを診る医師にお願いしたいこと"で始まる本書は、優しい口調で書かれてはいるが、実は氏から我々への最終通告ではないか。発達障害を抱えた子どもたちに接する機会のある者が、その障害について理解を深める努力をしないのであれば、もうこれ以上診療を続ける資格はない。そう叱咤された気がした。項目ごとにある箇条書きの要点、これが極めて明快だ。そして、文章の切れが良い。問題点と今やるべきことを、ずばずばと直球で投げ込んでくる。素晴らしい個性を持ちながら、それを発揮するための社会性を獲得できず苦しんでいる子どもたち、大人たちがいる。だから、「様子をみましょう」と言わないでほしい。氏の強い気持ちがズンと腹に響いた(推薦のことばより)。

主な内容

2009・10

金原出版 〒113-8687 東京都文京区湯島2-31-14 TEL03-3811-7184(営業部直通) FAX03-3813-0288
振替00120-4-151494 ホームページ http://www.kanehara-shuppan.co.jp/

CLINICAL REPORT

AMERICAN JOURNAL OF medical genetics PART A

Aberrant Methylation of H19-DMR Acquired After Implantation Was Dissimilar in Soma Versus Placenta of Patients With Beckwith–Wiedemann Syndrome

Ken Higashimoto,[1] Kazuhiko Nakabayashi,[2] Hitomi Yatsuki,[1] Hokuto Yoshinaga,[1] Kosuke Jozaki,[1] Junichiro Okada,[3] Yoriko Watanabe,[3] Aiko Aoki,[4] Arihiro Shiozaki,[4] Shigeru Saito,[4] Kayoko Koide,[1] Tsunehiro Mukai,[5] Kenichiro Hata,[2] and Hidenobu Soejima[1]*

[1]Division of Molecular Genetics & Epigenetics, Department of Biomolecular Sciences, Faculty of Medicine, Saga University, Saga, Japan

[2]Department of Maternal–Fetal Biology, National Research Institute for Child Health and Development, Setagaya, Tokyo, Japan

[3]Department of Pediatrics, Kurume University, Kurume, Japan

[4]Department of Obstetrics and Gynecology, University of Toyama, Toyama, Japan

[5]Nishikyushu University, Kanzaki, Saga, Japan

Received 7 October 2011; Accepted 19 January 2012

Gain of methylation (GOM) at the H19 differentially methylated region (H19-DMR) is one of several causative alterations in Beckwith–Wiedemann syndrome (BWS), an imprinting-related disorder. In most patients with epigenetic changes at H19-DMR, the timing of and mechanism mediating GOM is unknown. To clarify this, we analyzed methylation at the imprinting control regions of somatic tissues and the placenta from two unrelated, naturally conceived patients with sporadic BWS. Maternal H19-DMR was abnormally and variably hypermethylated in both patients, indicating epigenetic mosaicism. Aberrant methylation levels were consistently lower in placenta than in blood and skin. Mosaic and discordant methylation strongly suggested that aberrant hypermethylation occurred after implantation, when genome-wide de novo methylation normally occurs. We expect aberrant de novo hypermethylation of H19-DMR happens to a greater extent in embryos than in placentas, as this is normally the case for de novo methylation. In addition, of 16 primary imprinted DMRs analyzed, only H19-DMR was aberrantly methylated, except for *NNAT* DMR in the placental chorangioma of Patient 2. To our knowledge, these are the first data suggesting when GOM of H19-DMR occurs.

Key words: Beckwith–Wiedemann syndrome; H19-DMR; aberrant DNA methylation; after implantation

How to Cite this Article:
Higashimoto K, Nakabayashi K, Yatsuki H, Yoshinaga H, Jozaki K, Okada J, Watanabe Y, Aoki A, Shiozaki A, Saito S, Koide K, Mukai T, Hata K, Soejima H. 2012. Aberrant methylation of H19-DMR acquired after implantation was dissimilar in soma versus placenta of patients with Beckwith–Wiedemann syndrome.
Am J Med Genet Part A 9999:1–6.

INTRODUCTION

Beckwith–Wiedemann syndrome (BWS) is an imprinting-related condition characterized by macrosomia, macroglossia, and abdominal wall defects (OMIM #130650). The relevant imprinted chromosomal region in BWS, 11p15.5, consists of two independent imprinted domains, *IGF2/H19* and *CDKN1C/KCNQ1OT1*. Imprinted genes within each domain are regulated by two imprinting control regions (ICR), the H19-differentially methylated region (DMR) or KvDMR1 [Weksberg et al., 2010]. Several causative alterations have been identified in patients with BWS: loss of methylation (LOM) at KvDMR1, gain of methylation (GOM) at H19-DMR, paternal uniparental disomy (UPD), *CDKN1C* mutations, and chromosomal abnormality involving 11p15 [Sasaki et al., 2007; Weksberg et al., 2010].

Additional supporting information may be found in the online version of this article.

Grant sponsor: Japan Society for the Promotion of Science; Grant number: 20590330; Grant sponsor: Ministry of Health, Labor, and Welfare; Grant sponsor: National Center for Child Health and Development.

*Correspondence to:
Hidenobu Soejima, Professor[Q1], Division of Molecular Genetics & Epigenetics, Department of Biomolecular Sciences, Faculty of Medicine, Saga University, 5-1-1 Nabeshima, Saga 849-8501, Japan.
E-mail: soejimah@med.saga-u.ac.jp

Published online 00 Month 2012 in Wiley Online Library (wileyonlinelibrary.com).
DOI 10.1002/ajmg.a.35335

Methylation of H19-DMR is erased in primordial germ cells (PGCs) but becomes reestablished during spermatogenesis [Li, 2002; Sasaki and Matsui, 2008]: this methylation regulates the expression of *IGF2* and *H19* by functioning as a chromatin insulator, restricting access to shared enhancers [Bell and Felsenfeld, 2000; Hark et al., 2000]. GOM on the maternal H19-DMR leads to expression of both *IGF2* alleles and silencing of both *H19* alleles. Dominant maternal transmissions of microdeletions and/or base substitutions within H19-DMR have recently been reported in a few patients of BWS with H19-DMR GOM [Demars et al., 2010]. However, when and how the GOM on the maternal H19-DMR occurs is not clear.

Here, we found epigenetic mosaicism in two BWS patients. We also found that GOM at H19-DMR was discordant in blood and skin versus placenta; specifically, methylation levels were lower in placental samples. These findings strongly suggest that aberrant methylation of H19-DMR occurred after implantation. As a result, we expect aberrant de novo methylation happens to a greater extent in embryos than in placentas.

MATERIALS AND METHODS

Patients

Two unrelated patients with sporadic BWS, Patient 1 (BWS047) and Patient 2 (bwsh21-015), were delivered by cesarean in the third trimester of pregnancy. The mothers of both patients conceived naturally. Patient 1 and Patient 2 met clinical criteria for BWS as described by Elliott et al. [1994] and Weksberg et al. [2001], respectively (Table I). The placenta of Patient 1 was large and weighed 1,065 g, but was without any pathological abnormality. The placenta of Patient 2 was also large, weighing 1,620 g, and had an encapsulated placental chorangioma, as reported previously [Aoki et al., 2011]. The standard G-banding chromosome analysis using peripheral blood samples showed no abnormalities in either patient. This study was approved by the Ethics Committee for Human Genome and Gene Analyses of the Faculty of Medicine, Saga University.

Southern Blot Analysis

Genomic DNA was extracted from embryo-derived somatic tissues and the placentas of the patients (Fig. 1). Methylation-sensitive Southern blots with *Bam*HI and *Not*I were employed for KvDMR1, and blots with *Pst*I and *Mlu*I were employed for H19-DMR, as described previously [Soejima et al., 2004]. Band intensity was measured using the FLA-7000 fluoro-image analyzer (Fujifilm[Q2], Japan). The methylation index (MI, %) was then calculated (Fig. 1). Southern blots with *Apa*I were used to identify the microdeletion of H19-DMR as described previously [Sparago et al., 2004].

Bisulfite Sequencing and Combined Bisulfite Restriction Analysis (COBRA)

Bisulfite sequencing covering the sixth CTCF binding site (CTS6) was performed. For COBRA, PCR products of each primary imprinted DMR were digested with the appropriate restriction endonucleases and were then separated using the MultiNA Microchip Electrophoresis System (Shimazdu, Japan). The methylation index was also calculated. All PCR primer sets used in this study have been listed in Supplementary Table SI (See Supporting Information online).

DNA Polymorphism Analyses

For quantitative polymorphism analyses, tetranucleotide repeat markers (*D11S1997* and *HUMTH01*) and a triplet repeat marker (*D11S2362*) from 11p15.4–p15.5 were amplified and separated by electrophoresis on an Applied Biosystems 3130 genetic analyzer (Applied[Q3] Biosystems); data were quantitatively analyzed with the GeneMapper software. The peak height ratios of paternal allele to maternal allele were calculated. A single nucleotide polymorphism (SNP) for the *Rsa*I recognition site in *H19* exon 5 (rs2839703) was also quantitatively analyzed using hot-stop PCR [Uejima et al., 2000]. Band intensity was measured using the FLA-7000 fluoro-image analyzer (Fujifilm).

Mutation Search of H19-DMR

To search for mutations in the binding sites of CTCF, OCT4, and SOX2, we sequenced a genomic region in and around H19-DMR, which included seven CTCF-binding sites, three OCT4 sites, and one SOX2 site.

TABLE I. Clinical Information of BWS Patients

Patient ID	Conception	Birth weight (gestational age)	Clinical features	Karyotype	Placental weight and pathology	Placental–fetal weight ratio
Patient 1 (BWS047)	Natural	4,506 g (36w2d)	Macrosomia macroglossia abdominal wall defect hypoglycemia	46,XY	1,065 g no pathological findings	0.236
Patient 2 (bwsh21-015)	Natural	2,540 g (33w5d)	Macrosomia macroglossia hypoglycemia renal malformation hepatosplenomegaly	46,XX	1,620 g placental chorangioma	0.638

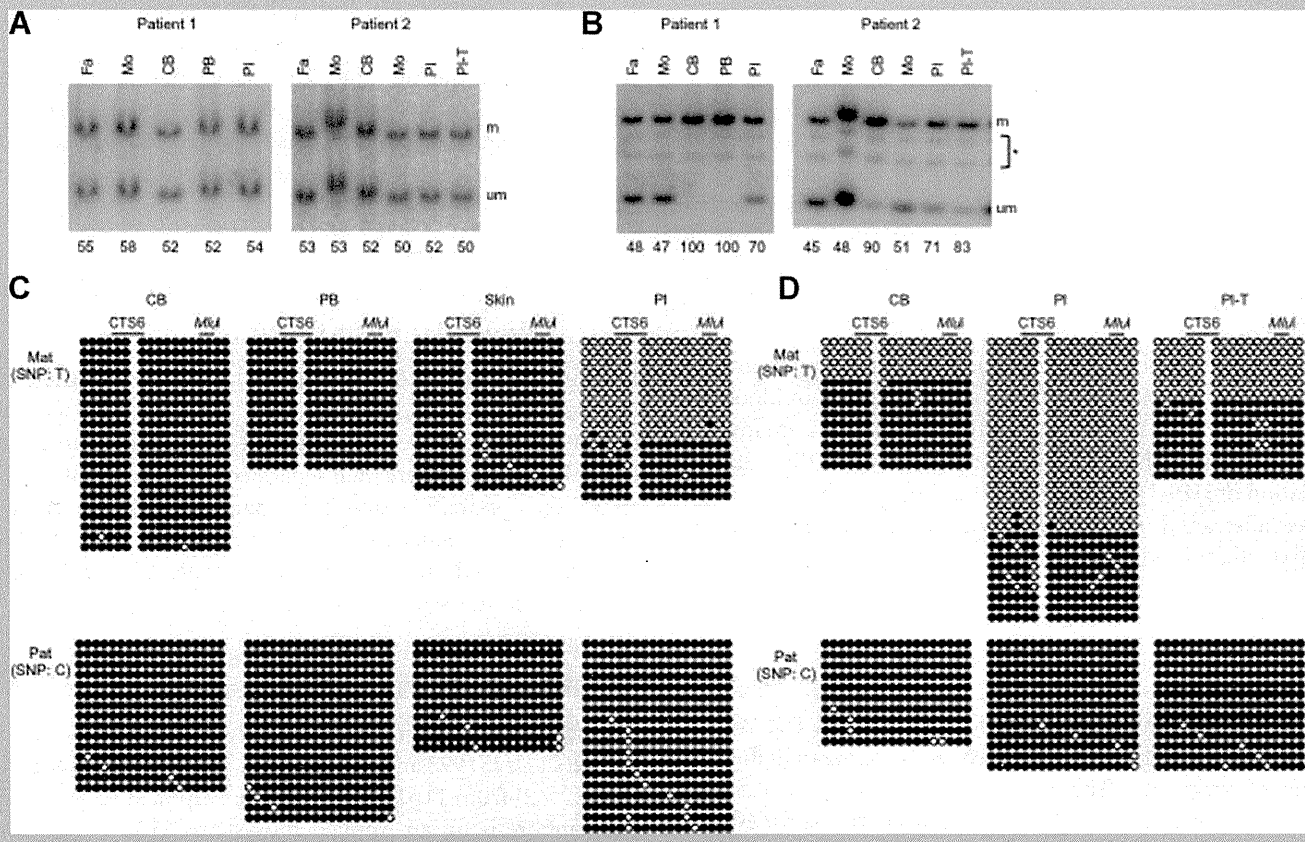

FIG. 1. Methylation analyses of KvDMR1 and H19-DMR. A: Methylation-sensitive Southern blots for KvDMR1. Genomic DNA was extracted from the cord blood, peripheral blood, skin, and placenta of Patient 1 and from the cord blood, placenta, and placental chorangioma of Patient 2. Methylation at KvDMR1 was normal in all samples analyzed. Methylation indices (MI, %) are shown under the figure. B: Methylation-sensitive Southern blots for H19-DMR. The MIs of blood samples were higher than the MIs of placental samples. MI was calculated using the equation $[M/(M+U)] \times 100$, where M is the intensity of the methylated band and U is the intensity of the unmethylated band. C: Bisulfite sequencing of H19-DMR in Patient 1. The two parental alleles were distinguishable by differences in SNPs. Both parental alleles were completely methylated in the cord blood, peripheral blood, and skin samples, and the maternal allele, which is normally unmethylated, was partially methylated in the placenta. D: Bisulfite sequencing of H19-DMR in Patient 2. Methylation of the maternal allele was higher in the cord blood than in the placenta or placental chorangioma. These results were consistent with the results of the Southern blot analysis. We confirmed complete methylation of paternal H19-DMR alleles and complete demethylation of maternal H19-DMR alleles in four normal control placentas that were heterozygous for identifiable SNPs (data not shown). Fa, father; Mo, mother; CB, cord blood; PB, peripheral blood; Pl, placenta; Pl-T, placental chorangioma; m, methylated band; um, unmethylated band; *, nonspecific bands; Mat, maternal allele; Pat, paternal allele; CTS6, sixth CTCF binding site; *MluI*, a restriction site approximately 80 bp downstream of CTS6 assayed by methylation-sensitive Southern blot and COBRA.

RESULTS

We first examined the methylation status of the two ICRs, KvDMR1, and H19-DMR, at 11p15.5 using methylation-sensitive Southern blot analysis. Methylation at KvDMR1 was normal in all samples collected (Fig. 1A); however, methylation at H19-DMR was aberrant (Fig. 1B). In Patient 1, hypermethylation at H19-DMR was complete in cord blood and peripheral blood samples (MI = 100%), and hypermethylation in the placenta was partial (MI = 70%). In Patient 2, H19-DMR was partially hypermethylated in cord blood (MI = 90%) but less so in the placenta and placental chorangioma (MI = 71% and MI = 83%, respectively). For further investigation of differences in methylation between the patients' somatic tissues and placentas, the CTS6 site was subjected to bisulfite sequencing (Fig. 1C and D). We could distinguish the two parental alleles in each patient sample using informative SNPs (rs10732516 and rs2071094). The maternal allele, which is normally unmethylated, was completely methylated in the cord blood, peripheral blood, and skin from Patient 1. However, in placental samples from Patient 1, the maternal allele was only partially methylated: 36% of all CpGs analyzed were methylated. Similar results were observed in Patient 2: the maternal allele in the cord blood was 68% methylated; however, the maternal allele was only 31% and 55% methylated in the placenta and chorangioma samples, respectively. The paternal alleles, which are normally fully methylated, were fully methylated in all samples. These findings supported the results of the Southern blots. Furthermore, we could not find any microdeletions or mutations in or around H19-DMR,

including seven CTCF-binding sites, three OCT4 sites, and one SOX2 site, indicating that there was no genetic cause of the hypermethylation (Fig. 2A and data not shown).

Next, we analyzed polymorphic markers at 11p15.4–p15.5 to determine whether copy number abnormalities or paternal UPD might be involved in these BWS patients. Although smaller PCR products were more easily amplified, paternal–maternal allele ratios in blood samples were between 0.92 and 1.33, indicating that both parental alleles were equally represented in both patients (Fig. 2B). Therefore, we could rule out copy number abnormality and paternal UPD within the patients' blood. We also investigated maternal contamination in the placenta. *D11S1997* and *HUMTH01* for Patient 1 and the *RsaI* polymorphism in *H19* (rs2839703) for Patient 2 were used for this investigation because the mothers were expected to be homozygous for such polymorphisms. Thus, we investigated contamination of our samples by assessing the homozygosity of the polymorphisms in the mothers. The paternal–maternal ratios in Patient 1 were 0.94 and 1.03, indicating an equal contribution of both parental alleles and suggesting no contamination (Fig. 2B). In Patient 2, the ratios were 0.77 and 0.78 in the placenta and chorangioma, respectively, suggesting a small amount of contamination (Fig. 2C). However, such contamination was too

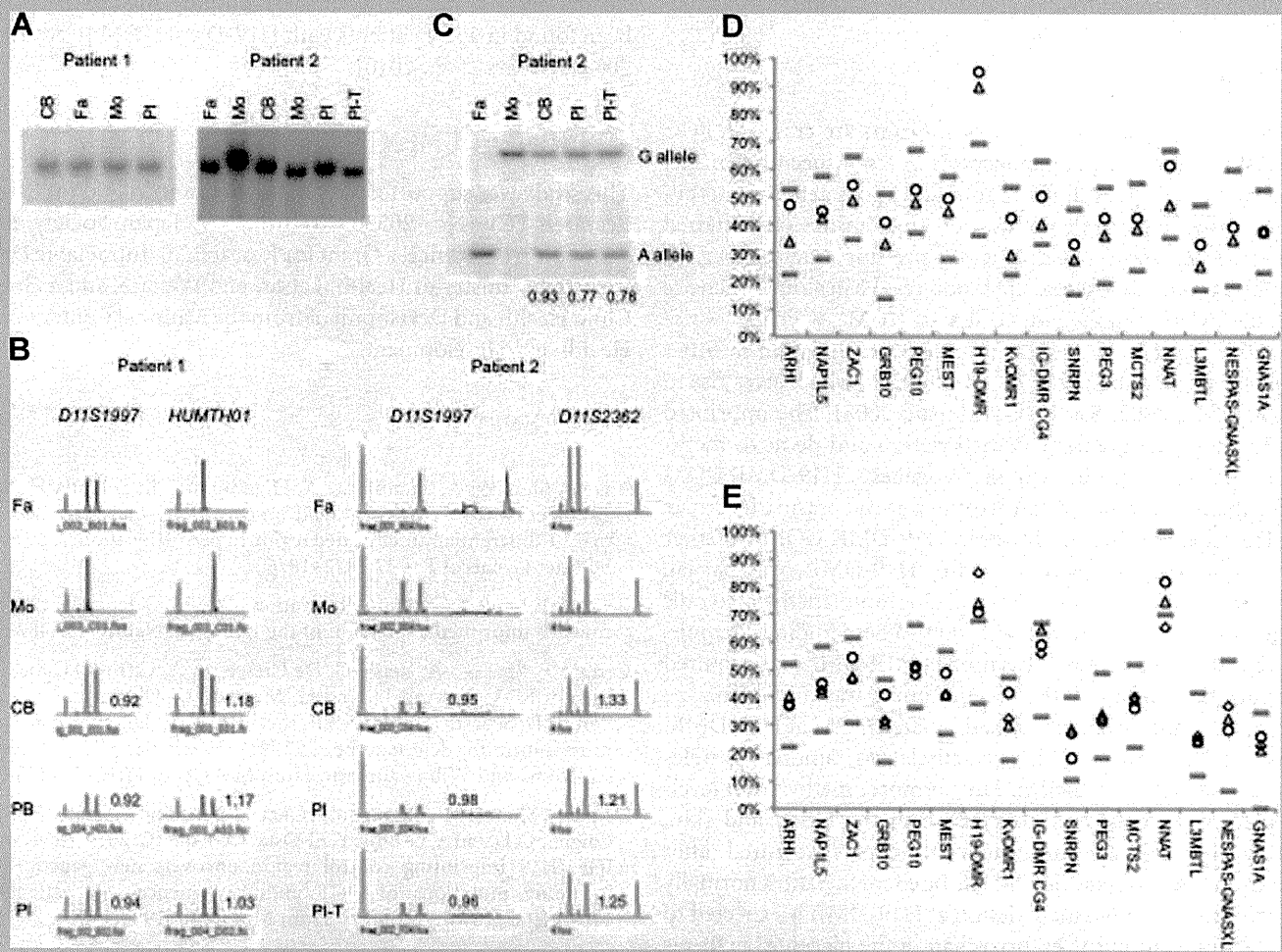

FIG. 2. Microdeletion analysis of H19-DMR, polymorphism analyses, and COBRA of primary imprinted DMRs in embryo-derived and placental samples. A: Southern blots identifying a microdeletion of H19-DMR. A genomic fragment (7.7 kb) generated by *ApaI* digestion, which included the entire H19-DMR, was evident in all samples, indicating that there was no microdeletion in this DMR. B: Microsatellite markers at 11p15.4–p15.5. The peak heights associated with each parental allele in all samples were quantitatively analyzed. The results indicated that both parental alleles were present and equally represented. C: Hot-stop PCR of an *RsaI* polymorphic site in Patient 2. The ratios of paternal allele to maternal allele are shown under the figure. Although the ratios in the placenta and placental chorangioma are lower than in the cord blood, suggesting a small amount of maternal contamination, this was not enough to affect the results of the methylation analyses. COBRA of cord blood (D) and placentas (E), demonstrating that H19-DMR was hypermethylated. CTS6 is contained within H19-DMR. Methylation at other DMRs was normal in all samples, except for methylation at NNAT, which was aberrant in the placental chorangioma. Cord blood and placentas from 24 normal individuals were used as controls. The upper limit of normal methylation was defined as the higher of these two values: (1) the average of controls + 3 SD, or (2) the average + 15%. Similarly, the lower limit of normal methylation was definite as the lower of these two values: (1) the average of controls − 3 SD, or (2) the average − 15%. The upper and lower limits are indicated by gray bars. ○: Patient 1; : Patient 2; ◇: placental chorangioma of Patient 2.

small to affect the results of the methylation analyses. In addition, sequence analysis did not show any mutations in *CDKN1C* (data not shown). These findings indicated that H19-DMR was aberrantly hypermethylated in both BWS patients and their associated placentas, but the aberrant methylation was consistently lower in the placenta, and that the H19-DMR GOM was strictly an isolated epimutation.

Finally, we analyzed the methylation status of 16 primary imprinted DMRs scattered throughout the genome-using COBRA (Fig. 2D and E). Only H19-DMR showed aberrant methylation among all primary DMRs in all samples, except for NNAT DMR, which was abnormal only in the placental chorangioma, indicating that the *IGF2/H19* imprinted domain was targeted for aberrant methylation in both somatic tissues and the placenta.

DISCUSSION

Methylation associated with parental imprints are erased in PGC and reestablished during gametogenesis in a sex-specific manner. The paternal pronucleus in the zygote undergoes active demethylation; extensive passive demethylation then ensues on maternal and paternal chromosomes during the pre-implantation period. After implantation, de novo methylation results in a rapid increase in DNA methylation in the inner cell mass (ICM), which gives rise to the entire embryo; in contrast, de novo methylation is either inhibited or not maintained in the trophoblast, which gives rise to the placenta [Li, 2002; Sasaki and Matsui, 2008]. The imprinted DMRs, however, escape these demethylation and de novo methylation events that occur in early embryogenesis. H19-DMR GOM in BWS patients is considered an error in imprint erasure in female PGCs [Horsthemke, 2010]. However, H19-DMR GOM, whether with or without microdeletions within H19-DMR, was partial, indicating a mosaic of normal cells and aberrantly methylated cells [Sparago et al., 2007; Cerrato et al., 2008]. These findings demonstrated that aberrant hypermethylation at H19-DMR was acquired after fertilization, although the precise timing was unknown.

Both participants in this study had isolated GOM at H19-DMR. The partial and variable hypermethylation among samples suggested epigenetic mosaicism. Furthermore, methylation levels in the placentas were lower than those in the blood and skin, suggesting that the aberrant methylation was acquired after implantation—when genome-wide de novo methylation normally occurs. Aberrant de novo methylation at H19-DMR is expected to be more widespread in the embryo than in the placenta, as this is normally the case for de novo methylation [Li, 2002; Sasaki and Matsui, 2008]; this disparity in efficiency could lead to the discordance between hypermethylation in trophoblast-derived placenta and that in embryo-derived blood and skin. This hypothesis is supported by a mouse experiment in which a mutant maternal allele harboring a deletion of four CTCF binding sites was hypomethylated in oocytes and blastocysts, yet was highly methylated after implantation [Engel et al., 2006]. To our knowledge, this is the first evidence demonstrating that aberrant hypermethylation of maternal H19-DMR is acquired after implantation in humans.

We found that of 16 primary imprinted DMRs analyzed, only H19-DMR showed aberrant methylation; even methylation at IG-DMR CG4, another paternally methylated, primary imprinted DMR, was normal in our patients. Although we only studied two patients, this finding indicated that the *IGF2/H19* imprinted domain in both the embryo and placenta was more susceptible than other imprinted domains to aberrant methylation acquired after implantation.

In conclusion, we found that methylation of H19-DMR was discordant in embryo-derived somatic tissue and placenta, strongly suggesting that the aberrant de novo methylation occurred after implantation. However, the precise mechanism of isolated H19-DMR GOM is still unknown. Since no mutations in *CTCF*, an important trans-acting imprinting factor, were found in these patients with isolated GOM at H19-DMR, the potential for mutations in the OCT and SOX transcription factors should be investigated because mutations of OCT-binding sites have previously been found in a few patients with H19-DMR GOM [Cerrato et al., 2008; Demars et al., 2010].

ACKNOWLEDGMENTS

This study was supported, in part, by a Grant-in-Aid for Scientific Research (C) (No. 20590330) from the Japan Society for the Promotion of Science, a Grant for Research on Intractable Diseases from the Ministry of Health, Labor, and Welfare, and a Grant for Child Health and Development from the National Center for Child Health and Development.

REFERENCES

Aoki A, Shiozaki A, Sameshima A, Higashimoto K, Soejima H, Saito S. 2011. Beckwith–Wiedemann syndrome with placental chorangioma due to H19-differentially methylated region hypermethylation: A case report. J Obstet Gynaecol Res 37:1872–1876.

Bell AC, Felsenfeld G. 2000. Methylation of a CTCF-dependent boundary controls imprinted expression of the Igf2 gene. Nature 405:482–485.

Cerrato F, Sparago A, Verde G, De Crescenzo A, Citro V, Cubellis MV, Rinaldi MM, Boccuto L, Neri G, Magnani C, D'Angelo P, Collini P, Perotti D, Sebastio G, Maher ER, Riccio A. 2008. Different mechanisms cause imprinting defects at the IGF2/H19 locus in Beckwith–Wiedemann syndrome and Wilms' tumour. Hum Mol Genet 17:1427–1435.

Demars J, Shmela ME, Rossignol S, Okabe J, Netchine I, Azzi S, Cabrol S, Le Caignec C, David A, Le Bouc Y, El-Osta A, Gicquel C. 2010. Analysis of the IGF2/H19 imprinting control region uncovers new genetic defects, including mutations of OCT-binding sequences, in patients with 11p15 fetal growth disorders. Hum Mol Genet 19:803–814.

Elliott M, Bayly R, Cole T, Temple IK, Maher ER. 1994. Clinical features and natural history of Beckwith–Wiedemann syndrome: Presentation of 74 new cases. Clin Genet 46:168–174.

Engel N, Thorvaldsen JL, Bartolomei MS. 2006. CTCF binding sites promote transcription initiation and prevent DNA methylation on the maternal allele at the imprinted H19/Igf2 locus. Hum Mol Genet 15:2945–2954.

Hark AT, Schoenherr CJ, Katz DJ, Ingram RS, Levorse JM, Tilghman SM. 2000. CTCF mediates methylation-sensitive enhancer-blocking activity at the H19/Igf2 locus. Nature 405:486–489.

Horsthemke B. 2010. Mechanisms of imprint dysregulation. Am J Med Genet C Semin Med Genet 154C:321–328.

Li E. 2002. Chromatin modification and epigenetic reprogramming in mammalian development. Nat Rev Genet 3:662–673.

Sasaki H, Matsui Y. 2008. Epigenetic events in mammalian germ-cell development: Reprogramming and beyond. Nat Rev Genet 9:129–140.

Sasaki K, Soejima H, Higashimoto K, Yatsuki H, Ohashi H, Yakabe S, Joh K, Niikawa N, Mukai T. 2007. Japanese and North American/European patients with Beckwith–Wiedemann syndrome have different frequencies of some epigenetic and genetic alterations. Eur J Hum Genet 15: 1205–1210.

Soejima H, Nakagawachi T, Zhao W, Higashimoto K, Urano T, Matsukura S, Kitajima Y, Takeuchi M, Nakayama M, Oshimura M, Miyazaki K, Joh K, Mukai T. 2004. Silencing of imprinted CDKN1C gene expression is associated with loss of CpG and histone H3 lysine 9 methylation at DMR-LIT1 in esophageal cancer. Oncogene 23:4380–4388.

Sparago A, Cerrato F, Vernucci M, Ferrero GB, Silengo MC, Riccio A. 2004. Microdeletions in the human H19 DMR result in loss of IGF2 imprinting and Beckwith–Wiedemann syndrome. Nat Genet 36:958–960.

Sparago A, Russo S, Cerrato F, Ferraiuolo S, Castorina P, Selicorni A, Schwienbacher C, Negrini M, Ferrero GB, Silengo MC, Anichini C, Larizza L, Riccio A. 2007. Mechanisms causing imprinting defects in familial Beckwith–Wiedemann syndrome with Wilms' tumour. Hum Mol Genet 16:254–264.

Uejima H, Lee MP, Cui H, Feinberg AP. 2000. Hot-stop PCR: A simple and general assay for linear quantitation of allele ratios. Nat Genet 25: 375–376.

Weksberg R, Nishikawa J, Caluseriu O, Fei YL, Shuman C, Wei C, Steele L, Cameron J, Smith A, Ambus I, Li M, Ray PN, Sadowski P, Squire J. 2001. Tumor development in the Beckwith–Wiedemann syndrome is associated with a variety of constitutional molecular 11p15 alterations including imprinting defects of KCNQ1OT1. Hum Mol Genet 10:2989–3000.

Weksberg R, Shuman C, Beckwith JB. 2010. Beckwith–Wiedemann syndrome. Eur J Hum Genet 18:8–14.

THE JOURNAL OF
Obstetrics and Gynaecology Research

doi:10.1111/j.1447-0756.2011.01654.x J. Obstet. Gynaecol. Res. Vol. 37, No. 12: 1872–1876, December 2011

Beckwith–Wiedemann syndrome with placental chorangioma due to H19-differentially methylated region hypermethylation: A case report

Aiko Aoki[1], Arihiro Shiozaki[1], Azusa Sameshima[1], Ken Higashimoto[2], Hidenobu Soejima[2] and Shigeru Saito[1]

[1]*Department of Obstetrics and Gynecology, University of Toyama, Toyama, and* [2]*Division of Molecular Genetics and Epigenetics, Department of Biomolecular Sciences, Faculty of Medicine, Saga University, Saga, Japan*

Abstract

Beckwith–Wiedemann syndrome (BWS) is a common overgrowth syndrome that involves abdominal wall defects, macroglossia, and gigantism. It is sometimes complicated by placental tumor and polyhydramnios. We report a case of BWS, prenatally diagnosed with ultrasonography. A large and well-circumscribed tumor also existed on the fetal surface of the placenta, which was histologically diagnosed as chorangioma after delivery. Polyhydramnios was obvious and the fetal heart enlarged progressively during pregnancy. Because the biophysical profiling score dropped to 4 points at 33 weeks of gestation, we carried out cesarean section. By epigenetic analysis, H19-differentially methylated region hypermethylation was observed in the placental tumor, normal placental tissue, and cord blood mononuclear cells. This is the first report of BWS with placental tumor due to H19-differentially methylated region hypermethylation.

Key words: Beckwith–Wiedemann syndrome, epigenetic abnormality, H19-differentially methylated region, hypermethylation, placental chorangioma, prenatal diagnosis.

Introduction

The incidence of Beckwith–Wiedemann syndrome (BWS) is estimated to be 1 in 13 700 deliveries.[1] BWS presents characteristic findings, genetic abnormalities, and a higher risk of malignancies. To our knowledge, there are only four reports of BWS with placental chorangioma, but no report was supported by epigenetic analysis. This is the first report of BWS with placental chorangioma, biallelic expression of *IGF2*, and reduced *H19* expression.

Case Report

A 27-year-old woman had an uneventful pregnancy (gravida 0, para 0) until 29 weeks of gestation. Assisted reproductive technology had not been performed. She complained of increased abdominal circumference and a sense of oppression at 29 weeks and 3 days into her pregnancy. Transabdominal sonography showed that the fetus was large for the gestational age. Additionally, a large and well-circumscribed placental tumor measuring about 12 cm in diameter and polyhydramnios were observed. She was diagnosed with preterm labor and was transferred to our hospital. Ultrasonography showed fetal macroglossia (Fig. 1a), enlargement of the liver (Fig. 1b) and the kidneys (Fig. 1c,d), and a large and well-circumscribed placental tumor (Fig. 1e). These clinical physical features suggested a prenatal diagnosis of BWS. Mild mitral and tricuspid regurgitation appeared in the fetal heart at 32 weeks of gestation, and became worse at 33 weeks of gestation. At 33 weeks and 5 days of gestation, biophysical profiling score was dropped to 4 points, and therefore a cesarean section

Received: February 3 2011.
Accepted: March 18 2011.
Reprint request to: Professor Shigeru Saito, Department of Obstetrics and Gynecology, University of Toyama, 2630 Sugitani, Toyama 930-0194, Japan. Email: s30saito@med.u-toyama.ac.jp

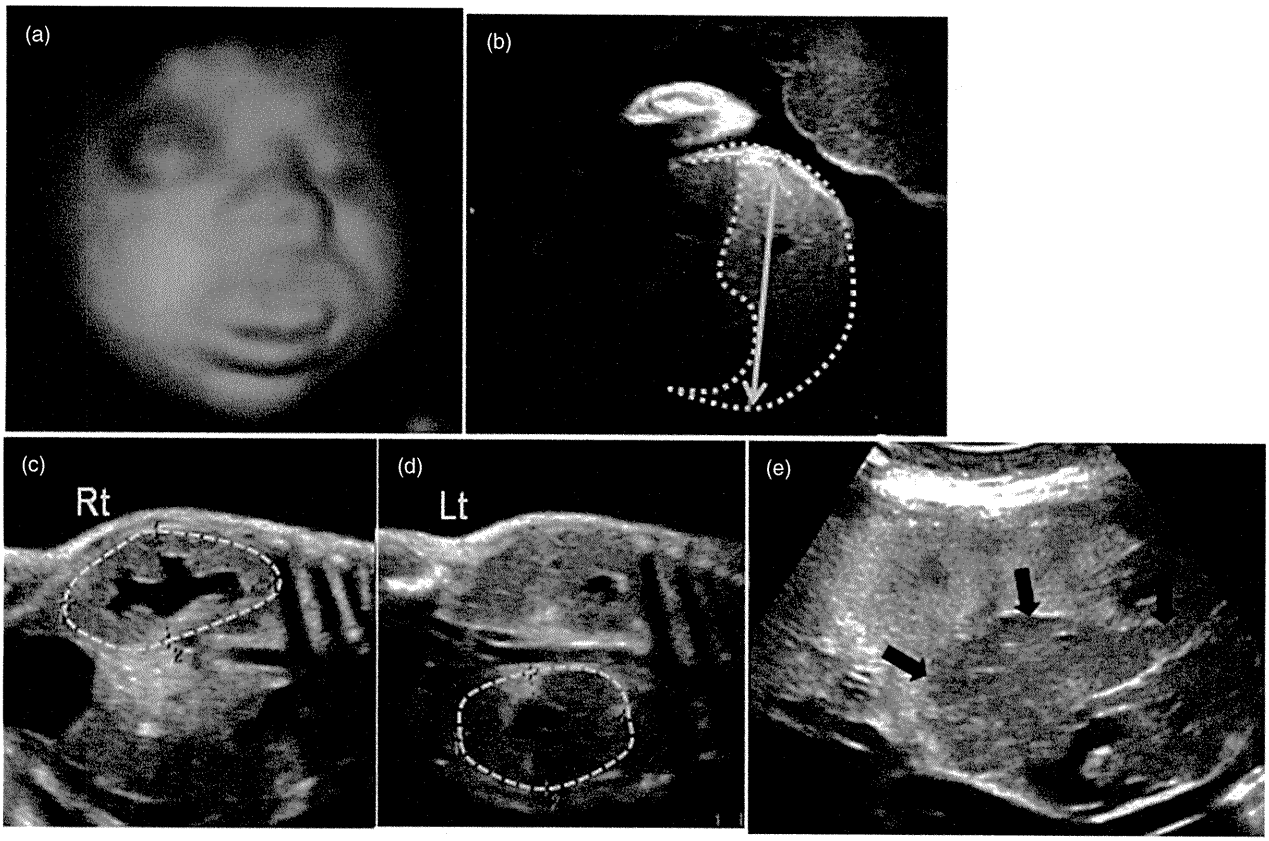

Figure 1 (a–e) Fetal and placental findings. Characteristic findings were seen using ultrasonography. (a) Macroglossia. (b) Hepatomegaly, measuring 87 mm (normal range at 29 weeks: 39 mm). (c,d) Enlarged kidneys, measuring 60 × 32 mm in right side, and 50 × 37 mm in the left side (normal range at 29 weeks: 28 × 15 mm). (e) A large, well-circumscribed tumor (12 cm in diameter) was found on fetal side of the placenta (arrows).

was performed for non-reassuring fetal status. The female baby weighed 2540 g and umbilical arterial blood pH was 7.127. Apgar scores were 3 and 7 points at 1 and 5 min, respectively. The baby had solitary, purple-red focuses on the body, macroglossia, and distended abdomen. Blood test showed hyperleukocytosis (32 520/mm^3), anemia (9.0 g/dL), thrombocytopenia (5.8×10^4/mm^3), and coagulopathy (Table 1). Blood transfusion was done for continuous anemia and low platelet count. For persistent neonatal hypoglycemia (around 20 mg/dL), steroid and glucose were used to keep the blood sugar level normal. Although mitral and tricuspid valve regurgitations existed, the cardiac function was stable. The fetal heart became progressively enlarged on the 8th postnatal day, and the baby suddenly died of cardiogenic shock on the 64th postnatal day (Fig. 2).

Table 1 Coagulopathy in the neonatal blood test

Prothrombin time	45.4 s
Prothrombin time %	<20
International normalized ratio	4.52
Activated partial thromboplastin time	>100 s
Fibrinogen	<50 mg/dL
Fibrin degenerative product	109.9 μg/mL
D-Dimer	35.0 μg/mL

The weight of the placenta was 1620 g with a well-capsulated placental tumor measuring 12 cm on the fetal side of the placenta (Fig. 3a). Histological examination showed enlarged villi with an increased number of small blood vessels and the tumor was diagnosed with cellular placental chorangioma (Fig. 3b,c).

The epigenetic analysis after delivery of the cord blood, placenta, and a part of the placental tumor showed H19-differentially methylated region (DMR)

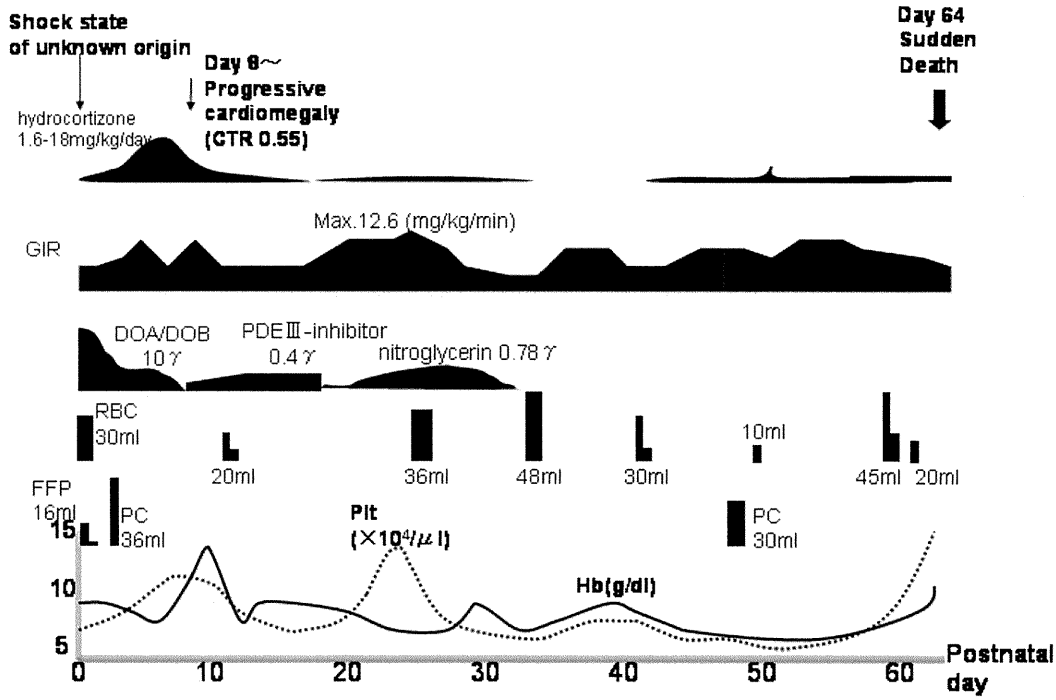

Figure 2 Neonatal clinical course. The baby went into a shock state 2 h after delivery, and was resuscitated with heart massage, cardiotonics and infusion of normal saline and sodium hydrogen carbonate. We performed a blood transfusion for continuous anemia and low platelet count. Because the glucose supply was not enough for persistent hypoglycemia, we administered steroids to keep the blood sugar level normal. The fetal heart was progressively enlarged on the 8th postnatal day, and the baby suddenly died of cardiogenic shock on the 64th postnatal day. CTR, cardiothoracic rate; DOA/DOB: dopamine/dobutamine; FFP, fresh frozen plasma; GIR, glucose infusion rate; Hb, hemoglobin; PC, platelet concentrates; PDE III-inhibitor, phosphodiesterase III inhibitor; Plt, platelet; RBC, red blood cell.

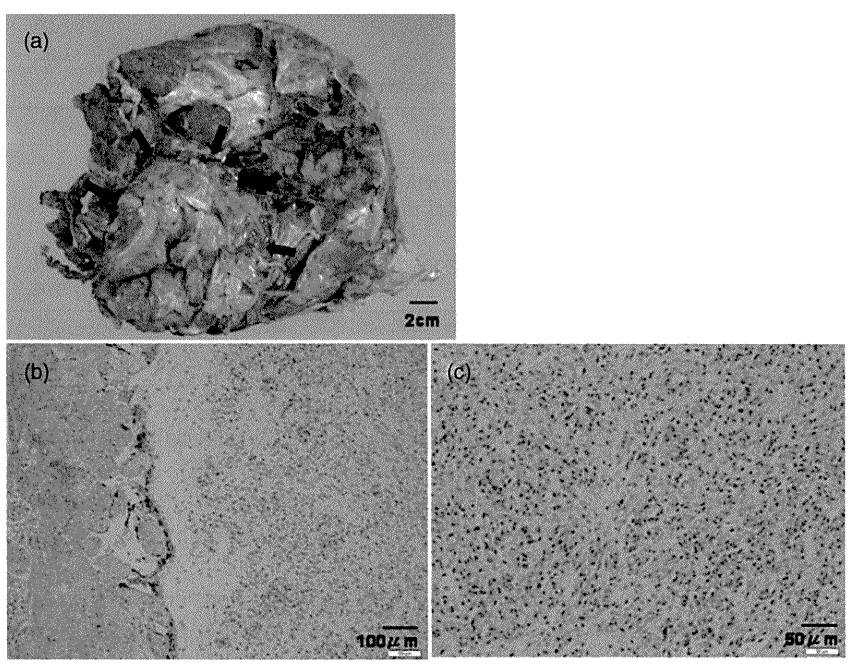

Figures 3 (a–c) Macroscopic and histological appearance of the placental tumor. (a) A well-circumscribed tumor (12.5 × 11.5 cm) was found on the fetal surface of the placenta (arrow). (b) Villi are enlarged and edematous (in the middle). (c) There is diffuse vascular proliferation in the enlarged villi, compatible with chorangioma.

hypermethylation. The parental blood tests showed no epigenetic abnormalities (Fig. 4). Another candidate methylation alteration site in BWS, KvDMR1, was normally methylated (data not shown). Genetic analyses ruled out paternal uniparental disomy of 11p15.5 and mutation of *CDKN1C* (data not shown).

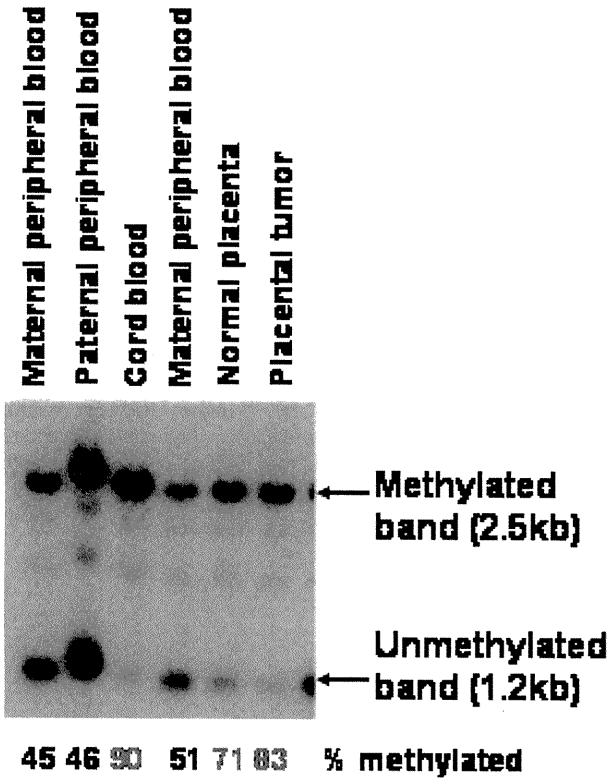

Figure 4 Epigenetic analysis. Quantity of H19-differentially methylated region (DMR) methylation status was determined by Southern blotting. Three micrograms of genomic DNA was digested with *Pst*I and methylation-sensitive *Mlu*I. The blot was probed by the PCR product, which was generated with a primer pair: 5′-CTCCGACTCCGTCTAAGGACA-3′ and 5′-GAGTGGAGACTGGCGAGTTTC-3′. KvDMR1 methylation status was also analyzed by Southern blotting with *Bam*HI and methylation-sensitive *Not*I. The blot was probed as previously described.[2] Band intensity obtained from Southern blotting was measured with a FLA-7000. The methylation index was calculated by (intensity of methylated band/[intensity of methylated band + intensity of unmethylated band]). H19-DMR hypermethylations are seen in the cord blood, normal placenta, and a part of the placental tumor (90%, 71%, 83%, respectively). Biallelic expression of *Igf2* and suppression of *H19* caused placentomegaly, macroglossia, visceromegaly and increased size for gestational age.

Discussion

Four BWS cases complicated with placental chorangioma have been reported,[3–6] but none was supported by epigenetic analysis. This is, to our knowledge, the first report proven to have epigenetic abnormality in BWS with placental chorangioma.

Chorangioma is asymptomatic when the size is smaller than 5 cm in diameter, but chorangiomas larger than 5 cm can cause some clinical problems, such as polyhydramnios, intrauterine fetal distress or death, fetal cardiac failure, neonatal anemia and thrombocytopenia, and disseminated intravascular coagulation, triggered by thromboplastic substances released from the small blood vessels in the chorangioma.[7] In our case, the tumor size was 12 cm and the features described above were observed.

Genomic imprinting is an epigenetic modification that inactivates one allele of a gene in a parent-of-origin-dependent manner.[8] Insulin-like growth factor 2 (*IGF2*)-*H19* imprinting control region (ICR), consisting of a methylation-sensitive chromatin insulator on chromosome 11p15.5, is responsible for epigenetic malformations in BWS.[9] In the *Igf2-H19* domain, especially in the placenta and tissues of endodermal origin, such as the liver, allele-specific gene expressions of parental origin are regulated by ICR located 2–4 kb upstream of the *H19* promoters. This region functions as a methylation-sensitive insulator that binds to CCCTC-binding factor (CTCF) on the unmethylated maternal allele. Alternatively, on the paternal allele, DNA methylation of ICR prevents CTCF binding, which permits access of the downstream enhancers to paternal *Igf2* promoters.[8]

In BWS cases, which have H19-DMR methylations in both paternal and maternal alleles (H19-DMR hypermethylation), the enhancers on the maternal allele activates *IGF2* promoters, leading to biallelic *IGF2* expression and the maternal copy of the *H19* gene is silenced because of expanded methylation to its promoter. Expression of imprinting gene, *IGF2*, depends on whether ICR is methylated or not, and loss of imprinting (LOI) of *IGF2* is associated with downregulation of *H19* expression, as previously reported.[10–12] Using epigenetic analysis, we could prove the existence of H19-DMR hypermethylation in the cord blood, placenta, and the placental tumor. Although we could not show biallelic *IGF2* expression because of homozygosity for *IGF2* polymorphism in the case (data not shown), H19-DMR hypermethylation would result in biallelic *IGF2* expression and associated reduced expression of *H19* due to the

reason mentioned above. In view of the potential function of *IGF2-H19*, these conditions led to cell proliferation and caused clinical appearances, such as macroglossia, visceromegaly (increased abdominal circumference), and the placental tumor. We explained to the mother that an occasional epigenetic abnormality (H19-DMR hypermethylation) caused BWS in the baby and that it would be extremely rare to recur in the next pregnancy.

References

1. Thorburn MJ, Wright ES, Miller CG, Smith-Read EH. Exomphalos-macroglossia-gigantism syndrome in Jamaican infants. *Am J Dis Child* 1970; **119**: 316–321.
2. Mitsuya K, Meguro M, Lee MP *et al. LIT1*, an imprinted antisense RNA in the human *KvLQT1* locus identified by screening for differentially expressed transcripts using monochromosomal hybrids. *Hum Mol Genet* 1999; **8**: 1209–1217.
3. Lage JM. Placentomegaly with massive hydrops of placental stem villi, diploid DNA content, and fetal omphaloceles: possible association with Beckwith–Wiedemann syndrome. *Hum Pathol* 1991; **22**: 591–597.
4. Drut RM, Drut R. Nonimmune fetal hydrops and placentomegaly: diagnosis of familial Wiedemann-Beckwith syndrome with trisomy 11p15 using FISH. *Am J Med Genet* 1996; **62**: 145–149.
5. Takayama M, Soma H, Yaguchi S *et al.* Abnormally large placenta associated with Beckwith–Wiedemann syndrome. *Gynecol Obstet Invest* 1986; **22**: 165–168.
6. Drut R, Drut RM, Toulouse JC. Hepatic hemangioendotheliomas, placental chorioangiomas, and dysmorphic kidneys in Beckwith–Wiedemann syndrome. *Pediatr Pathol* 1992; **12**: 197–203.
7. Fox H. Non-trophoblastic tumors of the placenta. In: Fox H (ed.). *Obstetrical and Gynecological Pathology*, 3rd edn. Philadelphia: Churchill Livingstone, 1987; 1030–1044.
8. Fowden AL, Sibley C, Reik W, Constancia M. Imprinted genes, placental development and fetal growth. *Horm Res* 2006; **65** (Suppl 3): 50–58.
9. Choufani S, Shuman C, Weksberg R. Beckwith–Wiedemann syndrome. *Am J Med Genet C Semin Med Genet* 2010 **154C**: 343–354.
10. Steenman MJ, Rainier S, Dobry CJ, Grundy P, Horon IL, Feinberg AP. Loss of imprinting of *IGF2* is linked to reduced expression and abnormal methylation of *H19* in Wilms' tumour. *Nat Genet* 1994; **7**: 433–439.
11. Bell AC, Felsenfeld G. Methylation of a CTCF-dependent boundary controls imprinted expression of the *Igf2* gene. *Nature* 2000; **405**: 482–485.
12. Hark AT, Schoenherr CJ, Katz DJ, Ingram RS, Levorse JM, Tilghman SM. CTCF mediates methylation-sensitive enhancer-blocking activity at the *H19/Igf2* locus. *Nature* 2000; **405**: 486–489.

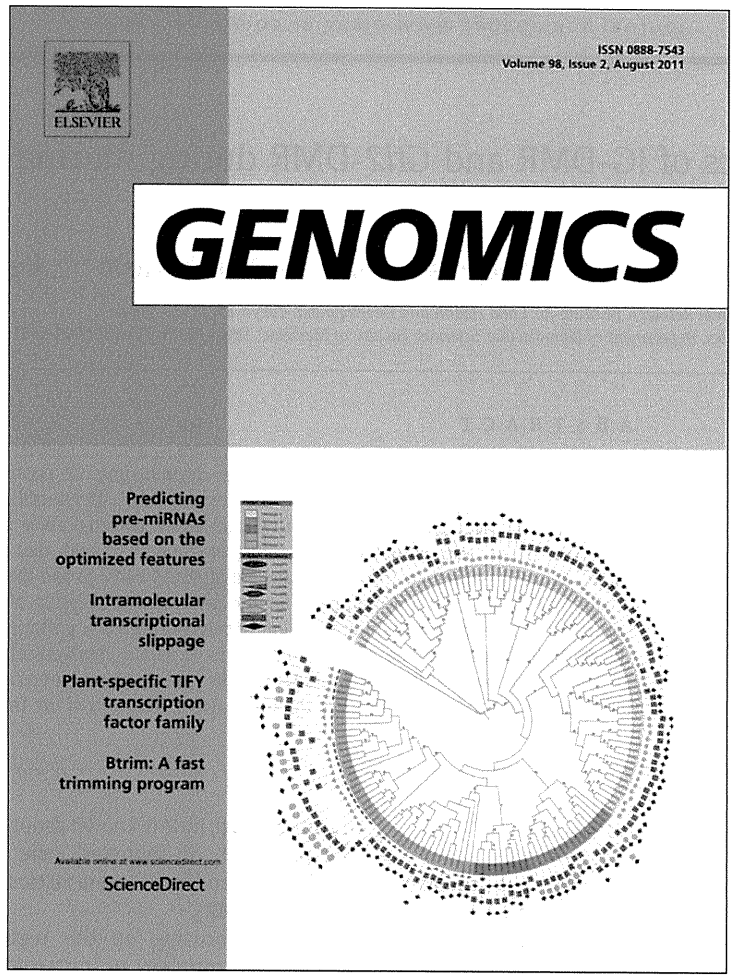

Genomics 98 (2011) 120–127

Contents lists available at ScienceDirect

Genomics

journal homepage: www.elsevier.com/locate/ygeno

Methylation dynamics of IG-DMR and *Gtl2*-DMR during murine embryonic and placental development

Shun Sato [a], Wataru Yoshida [a], Hidenobu Soejima [b], Kazuhiko Nakabayashi [a,*], Kenichiro Hata [a]

[a] Department of Maternal-Fetal Biology, National Research Institute for Child Health and Development, Tokyo 157-8535, Japan
[b] Division of Molecular Genetics and Epigenetics, Department of Biomolecular Sciences, Faculty of Medicine, Saga University, Saga 849-8501, Japan

ARTICLE INFO

Article history:
Received 5 December 2010
Accepted 12 May 2011
Available online 18 May 2011

Keywords:
Genomic imprinting
DNA methylation
IG-DMR
Gtl2-DMR

ABSTRACT

The *Dlk1-Dio3* imprinted domain on mouse chromosome 12 contains IG-DMR and *Gtl2*-DMR, whose methylation patterns are established in the germline and after fertilization, respectively. In this study, we determine that acquisition of DNA methylation at the paternal allele of the *Gtl2*-DMR is initiated after the blastocyst stage and completed by embryonic day 6.5, and that *Gtl2* (approved symbol: Meg3) is monoallelically expressed from the maternal allele as early as the blastocyst. Therefore, DNA methylation at the *Gtl2*-DMR is not a prerequisite for the imprinted expression of *Gtl2*, which may be involved in the control of proliferation and differentiation of cells during early gestation. We also reveal that a subregion of the IG-DMR exhibits tissue-specific differences in allelic methylation patterns. These results add to the growing body of knowledge elucidating the mechanism whereby parent-of-origin-dependent DNA methylation at the IG-DMR leads to the imprinted expression of the *Dlk1-Dio3* cluster.

1. Introduction

Genomic imprinting is an epigenetic mechanism that regulates transcription, whereby the expression of a subset of genes is limited to or biased towards one parental allele. To date, over one hundred imprinted genes have been identified in the mouse (http://www.har.mrc.ac.uk/research/genomic_imprinting). Imprinted genes tend to be clustered on the genome. One of the common features among imprinted loci is that such genomic intervals include one or more differentially methylated regions (DMRs), which exhibit parent-of-origin dependent DNA methylation patterns [1]. DMRs have been classified into two types according to the time at which their DNA methylation patterns are established. Primary (germline) DMRs harbor allelic DNA methylation inherited from the male or the female gamete. Secondary (post-zygotic) DMRs acquire parent-of-origin dependent methylation patterns after fertilization. In mice, germline DMRs are shown to be established during the oocyte growth stage (postnatal days 5 to 20) [2,3] or the prospermatogonia stage (embryonic days 14.5 to newborn) [4–6] by a DNMT3L-dependent mechanism [7–12]. Several germline DMRs have been shown to govern the imprinted expression of genes as well as the methylation of post-zygotic DMRs within chromosomal regions. These germline DMRs, known as imprinting control regions (ICRs), regulate these regions by *cis*-acting mechanisms. [13–15]. On the other hand, little is known about the function of secondary DMRs in the regulation of imprinted gene expression, as well as *cis*-acting mechanisms and *trans*-acting factors that establish DNA methylation at secondary DMRs.

Studies focusing on the regulatory functions of ICRs have revealed a number of different molecular mechanisms that underlie the coordinated and long-range regulation of imprinted genes. In the *H19/Igf2* domain, long range chromatin interactions mediated by CTCF between the primary *H19*-DMR and the secondary *Igf2*-DMRs play an integral role in the regulation of imprinted gene expression at this locus [13,16]. Another mechanism involves non-coding (nc) RNAs such as *Airn* in the *Igf2r* locus and *Kcnq1ot1* in the *Kcnq1* imprinted gene cluster. These ncRNAs are transcribed from ICRs and are shown to be functionally linked to the silencing of genes in *cis* through gene- and lineage-specific repressive chromatin modifications [14,17,18]. These two mechanisms are likely to be involved in the regulation of many other imprinted loci as well. However, the sequence of events leading to the establishment and maintenance of imprinted expression for a cluster of genes remains largely elusive for many imprinted loci.

The *Dlk1-Dio3* imprinting cluster on mouse distal chromosome 12 contains the intergenic germline-derived DMR (IG-DMR) and the *Gtl2*-DMR, whose methylation patterns are established in the germline and after fertilization, respectively [19,20]. The cluster consists of at least three paternally expressed protein-coding genes (*Dlk1*, *Rtl1*, and *Dio3*), and four maternally expressed ncRNAs (*Gtl2*, *Anti-Rtl1*, *Rian* and *Mirg*). The IG-DMR is shown to function as the ICR of this imprinted gene cluster [15,21]. A targeted disruption study of the IG-

* Corresponding author at: Department of Maternal-Fetal Biology, National Research Institute for Child Health and Development, 2-10-1 Okura, Setagaya, Tokyo 157-8535, Japan. Fax: +81 3 3417 2864.
E-mail address: knakabayashi@nch.go.jp (K. Nakabayashi).

0888-7543/$ – see front matter © 2011 Elsevier Inc. All rights reserved.
doi:10.1016/j.ygeno.2011.05.003

DMR [15] has revealed that the maternally inherited IG-DMR, which is unmethylated, is essential in the embryo to maintain the unmethylated status of the *Gtl2*-DMR, the expression of the ncRNAs, and the repression of the protein-coding genes, on the maternal allele. However, the principal mechanism whereby the allele-specific methylation at the IG-DMR leads to the imprinted expression of the cluster of genes on chromosome 12 is unknown. It has been also demonstrated that, in the placenta, the absence of the maternally inherited IG-DMR results in the activation of protein-coding genes but only partial repression of the ncRNAs, and leads to no phenotypic consequence [21]. Therefore, mechanisms underlying the imprinted expression of the maternally-expressed ncRNAs are different between the embryonic and the extra-embryonic tissue lineages.

Among known secondary DMRs, the *Gtl2*-DMR is unique in that it has been demonstrated to possess an essential long-range imprinting regulatory function. A neonatal patient showing a paternal uniparental disomy 14-like phenotype in the body but not in the placenta was identified to have a maternally-inherited heterozygous microdeletion that encompasses the *MEG3*-DMR (the human orthologue of the mouse *Gtl2*-DMR) but not the IG-DMR. In this patient, the maternal allele of *DLK1* has been shown to be reactivated [22]. Recent studies have used knockout mouse models with targeted deletions of the *Gtl2* locus, spanning the *Gtl2*-DMR. These studies have also suggested that *Gtl2* and/or *Gtl2*-DMR could regulate the expression of maternally expressed genes, indicating that the methylation of the *Gtl2*-DMR is a critical element in the *Dlk1-Dio3* imprinted domain [23,24]. In light of the critical roles that *Gtl2* and *Gtl2*-DMR may play in the imprinted regulation of this region, understanding the epigenetic mechanisms that govern them during early development is expected to further elucidate the mechanisms regulating the *Dlk1-Dio3* imprinted domain.

Recently, Stadtfeld et al. [25] reported that mouse induced pluripotent stem cells (iPSC) with repressed expression of maternally expressed ncRNAs in the *Dlk1-Dio3* domain contributed poorly to chimeras and failed to generate all-iPSC mice. In contrast, iPSCs with normal ncRNA expression patterns contributed to high-grade chimeras and produced all-iPSC mice. Hypermethylation of both the IG-DMR and the *Gtl2*-DMR was found to be associated with the reduced expression of ncRNAs in the iPSCs exhibiting poor contribution to chimeras [25]. This epimutation is considered to be caused by the iPSC reprogramming, rather than existing aberrant methylation patterns in the DMRs of the somatic cell of origin [25]. Therefore, a better understanding of the epigenetic regulation of these DMRs may eventually lead to improved reprogramming strategies of iPSC.

In this study, we determined the allelic DNA methylation patterns at the IG-DMR and the *Gtl2*-DMR, as well as the allelic expression patterns of *Dlk1* and *Gtl2* at early developmental stages (embryonic days 3.5 to 7.5) in embryonic and extra-embryonic tissues.

2. Results

2.1. Developmental dynamics of allelic DNA methylation patterns at IG- and Gtl2-DMRs in sperm, blastocysts, and post-implantation embryos

We examined allelic DNA methylation patterns at the IG-DMR and the *Gtl2*-DMR in whole embryos at embryonic day 3.5 (E3.5) and E5.5 as well as their methylation status in sperm. We regarded the genomic intervals defined by Kobayashi et al. [26] and Takada et al. [20] as the IG-DMR and the *Gtl2*-DMR, respectively. Three regions within the IG-DMR and the two regions within the *Gtl2*-DMR were chosen as targets for bisulfite sequencing (Fig. 1A). All five regions contain at least one single nucleotide polymorphism (SNP) between C57BL/6 (B6) and JF1/Ms (JF1) strains that can distinguish parental alleles in F1 hybrid materials (see details in Section 4.2 in the Materials and methods).

The IG-DMR was heavily methylated in all three regions (methylation percentage 81.3–95.8%) in sperm (Fig. 1B) as shown previously [20]. In blastocysts (E3.5), all three regions within the IG-DMR were maternally unmethylated (0–1.8%), yet paternally methylated (43.1–71.8%) (Fig. 1B). The observed levels of paternal methylation at E3.5 were significantly lower than those observed in sperm, implying that the paternal IG-DMR partially loses methylation at CpG dinucleotides after fertilization. This loss of methylation may be caused by the active and the passive demethylation of the paternal genome in pronucleus and preimplantation embryos, respectively [27,28]. At E5.5, the maternal allele of IG-DMR was found to be hypomethylated (1.9–18.3%), and the paternal allele to be hypermethylated (80.2–91.4%; Fig. 1B). The methylation level of the paternal allele was consistently higher at E5.5 than at E3.5. Additionally, it was almost fully methylated at E5.5 in all three regions examined, suggesting that de novo methylation events occur on the paternal allele of the IG-DMR during the developmental period between E3.5 and E5.5. These are the first results to illustrate the developmental dynamics of paternal methylation levels at the IG-DMR around the implantation period.

The differential methylation of the *Gtl2*-DMR on the paternal allele has been shown to be established in E13.5 embryos [20]. However, the post-zygotic stages at which the region's paternal methylation is initiated and completed remain unknown. Additionally, the relationship between the imprinted expression of *Gtl2* and DNA methylation at the *Gtl2*-DMR has not been elucidated. We confirmed that the *Gtl2*-DMR was unmethylated in sperm, and found that it was unmethylated on both parental alleles in blastocysts (Fig. 1B). In E5.5 embryos, the maternal allele remained hypomethylated (6.0 and 11.7%), while the paternal allele became partially methylated (55.2% in R4 and 42.7% in R5 regions) (Fig. 1B). In E6.5 and E7.5 embryos, the paternal allele of the *Gtl2*-DMR was found to be heavily methylated (75.8% or higher) (Fig. 1C). These data demonstrate that paternal methylation of the *Gtl2*-DMR is initiated after the blastocyst stage and is completed by E6.5 stage in the embryonic lineage.

2.2. Allelic DNA methylation patterns at IG- and Gtl2-DMRs in early and late gestational stages

It has been reported that, in both human and mouse placenta, the IG-DMR maintains its allele-specific methylation patterns, whereas the *Gtl2*-DMR does not show differential methylation between parental alleles [21,29,30]. To determine the developmental stage at which the allelic methylation patterns at the *Gtl2*-DMR diverge between embryonic and extra-embryonic lineages, we examined the DNA methylation status of the *Gtl2*-DMR as well as the IG-DMR in E6.5 and E7.5 tissues. In extra-embryonic tissues at both E6.5 and E7.5 stages, the *Gtl2*-DMR was partially methylated on both parental alleles, whereas its differential methylation was well maintained in embryonic tissues (Fig. 1C). The *Gtl2*-DMR was previously shown to be partially methylated on both parental alleles in late gestation (E16.5) placentas [21,29]. Our results demonstrate that the allelic methylation pattern observed in E16.5 placenta is already present in the extra-embryonic lineage at E6.5 stage.

Unexpectedly, we observed loss of differential methylation at the R2 and R3 regions within the IG-DMR in extra-embryonic tissues, although the R1 region maintained its differential methylation. The loss of differential methylation was more evident in E7.5 stage than in E6.5 stage (Fig. 1C). To assess whether the loss of differential methylation at the R2/R3 regions as well as the R4/R5 regions was specific to the extra-embryonic lineage, we examined the allelic methylation patterns of the R1–R5 regions in fetal tissues from late gestation time points. E16.5 skeletal muscle, E15.5 brain, and E16.5 liver were analyzed since they represent tissues derived from the

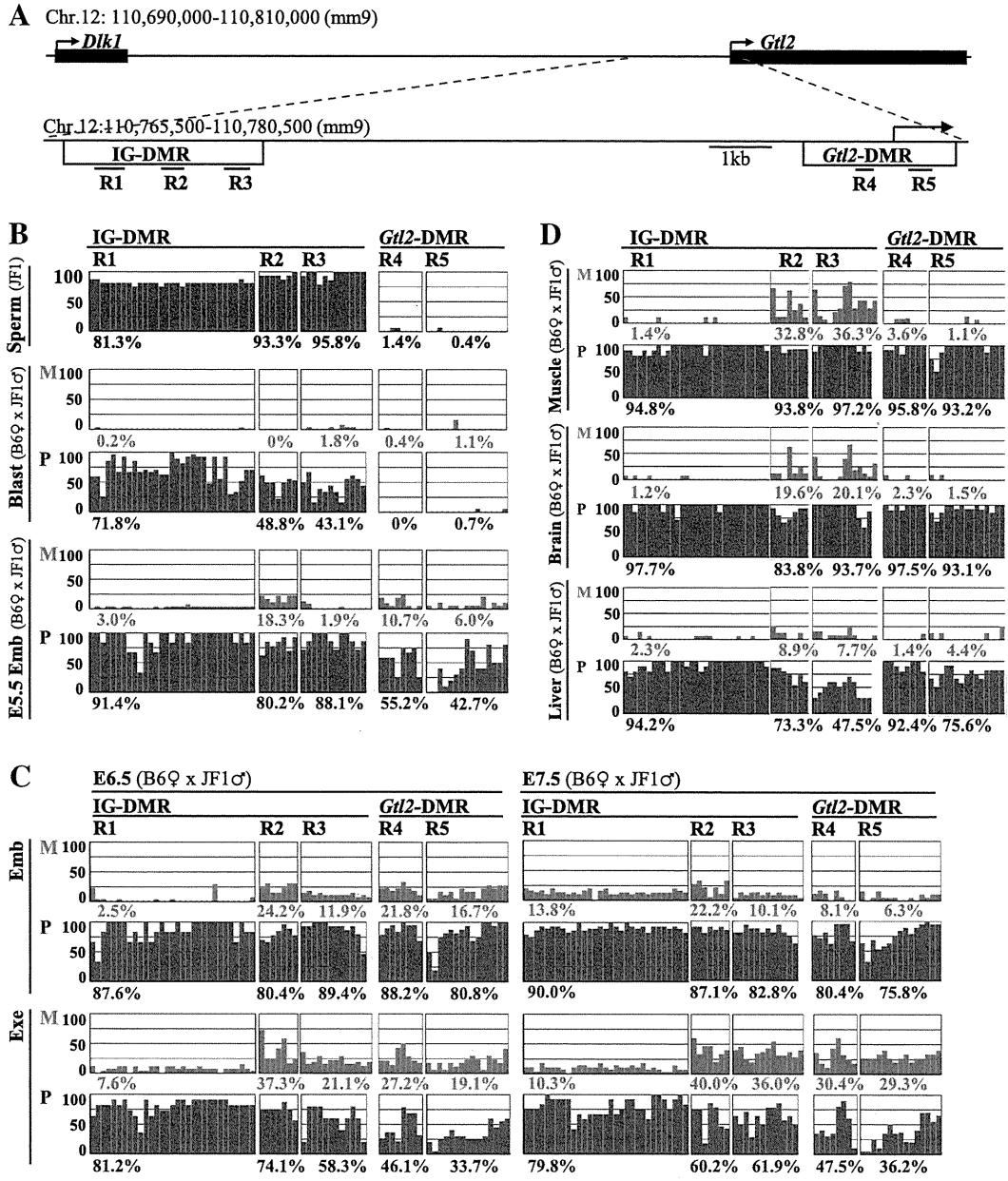

Fig. 1. Allelic DNA methylation patterns at the IG-DMR and the *Gtl2*-DMR during embryonic and extra-embryonic development. (A) A schematic diagram of the locus containing the IG-DMR and the *Gtl2*-DMR (shown as open boxes). The bars under the open boxes indicate the regions (R1–R5) analyzed by bisulfite sequencing. The arrow indicates the transcription start site of *Gtl2*. Scale bar = 1 kb. (B–D) Graphical representation of the methylation percentage at each CpG site in sperm, blastocysts at E3.5 (Blast), and embryos at E5.5 (E5.5_Emb) (B), in embryonic (Emb) and extra-embryonic (Exe) tissues at E6.5 and E7.5 (C), and in fetal tissues (E16.5 skeletal muscle, E15.5 brain, and E16.5 liver) (D). The vertical bars represent the percentage ratio of methylated cytosine at each CpG site, which were determined from the data of clone-based bisulfite sequencing (Supplementary Fig. 1). Overall methylation percentage for each region (the number of methylated CpGs per the number of total CpGs) is shown under each panel. As described in the Materials and Methods (Section 4.2), methylation percentage for each CpG site and each region was calculated using bisulfite sequencing data for a single sample (sperm and E15.5/16.5 fetal tissues) or two independent samples (E3.5 to E7.5 samples). M and P denote maternal and paternal alleles, respectively.

mesoderm, the ectoderm, and the endoderm, respectively. We found that differential methylation at the R1 region of the IG-DMR and the R4/R5 region of the *Gtl2*-DMR was strictly conserved. In contrast, differential methylation at the R2/R3 regions of the IG-DMR was partially lost to varying degrees in these tissues (Fig. 1D). Partial gain of methylation on the maternal allele (most notably observed in skeletal muscle) and partial loss of methylation on the paternal allele (most remarkably observed in the liver) were detected. Taken together, our data demonstrate that only a subregion of the IG-DMR containing the R1 region strongly maintains allele-specific differential methylation during embryonic development, whereas the rest of region containing the R2/R3 regions exhibits various tissue-specific allelic methylation patterns.

2.3. Allelic expression patterns of Dlk1 and Gtl2 during embryonic and extra-embryonic development

We subsequently assessed the expression levels and the allelic expression patterns of *Dlk1* and *Gtl2*. Although the expression of *Gtl2* is shown to be detectable as early as the pre-implantation stage [31], previous studies have not assessed the expression levels of these genes in a quantitative manner and have not determined their allelic expression patterns during early gestation (E3.5 to 7.5). Therefore, we performed both quantitative RT-PCR and pyrosequencing to quantify the allelic expression of these transcripts.

To determine the relative expression levels of *Gtl2* and *Dlk1*, quantitative RT-PCR was performed using E3.5 to E7.5 tissues and